Analysis of Bacterial Migration: I. Numerical Solution of Balance Equation

Paul D. Frymier, Roseanne M. Ford, and Peter T. Cummings
Dept. of Chemical Engineering, University of Virginia, Charlottesville, VA 22903

Chemotaxis describes the ability of motile bacteria to bias their motion in the direction of increasing gradients of chemicals, usually energy sources, known as attractants. In experimental studies of the migration of chemotactic bacteria, 1-D phenomenological cell balance equations (Rivero et al., 1989) have been used to quantitatively analyze experimental observations (Ford et al., 1991; Ford and Lauffenburger, 1991). While attractive for their simplicity and the ease of solution, they are limited in the strict mathematical sense to the situation in which individual bacteria are confined to motion in one dimension and respond to attractant gradients in one dimension only. Recently, Ford and Cummings (1992) reduced the general 3-D cell balance equation of Alt (1980) to obtain an equation describing the migration of a bacterial population in response to a 1-D attractant gradient. Solutions of this equation for single gradients of attractants are compared to those of 1-D balance equations, results from cellular dynamics simulations (Frymier et al., 1993), and experimental data from our laboratory for E. coli responding to α-methylaspartate. We also investigate two aspects of the experimentally derived expression for the tumbling probability: the effect of different models for the down-gradient swimming behavior of the bacteria and the validity of ignoring the temporal derivative of the attractant concentration.

Introduction

To quantitatively study the migration behavior of motile bacteria, recourse is made to cell balance equations which are analogous to mass balances in the study of mass transport. The ability of the bacteria to move in both random and coordinated fashions must be accounted for in the cell balance equations. It is therefore necessary to understand the microscopic dynamics of bacterial motion and incorporate this understanding in the population balance equations.

Much of the existing knowledge about the mechanisms of bacterial motion comes from the seminal work of Berg and coworkers (Berg and Brown, 1972; Brown and Berg, 1974; Berg, 1983) in which data on the three-dimensional trajectories of individual bacteria were acquired using the tracking microscope developed by Berg. We now briefly summarize this information. Peritrichous bacteria (of which *Escherichia coli* and *Salmonella typhimurium* are examples) move about in a fluid medium through the rotation of 6–8 flagella located around the periphery of the cell, alternating between two phases of motion. The direction of rotation can be clockwise or counterclockwise and determines the phase of motion of the bacteria. When they are rotating in a counterclockwise manner, the flagella form a coordinated bundle at the rear of the cell which propels the cell forward in an approximately straight path at a nearly constant speed. Counterclockwise rotation of the flagella and the resulting linear motion is called the "running" phase of bacterial motion. A cell typically displays this phase of motion for periods of 1 to 10 s. The average run time and the swimming speed of bacteria are important properties that characterize the transport rate of a population of bacteria. In between runs, the flagella will reverse and rotate clockwise, causing the flagellar bundle to unravel. As a result of the uncoordinated rotation of the flagella, the cell enters the "tum-

Correspondence concerning this article should be addressed to R. M. Ford.

bling" phase of motion in which it spins in place. The duration of the tumbling phase is on the order of one-tenth of a second. After the completion of the tumbling phase, the bacterium begins another run in a new direction. The path traced out by a bacterium as it alternates between the running phase and the tumbling phase is a random walk in a homogeneous fluid medium. The angle between the direction in which a bacterium is moving before tumbling and the direction of the run after executing a tumble is designated the turn angle. The turn angle distribution of a population is another important property used in describing its transport properties and has been measured for *E. coli* by Berg and Brown (1972) and Brown and Berg (1974).

As bacteria move about exploring their surroundings, they monitor changes in chemical concentrations through receptor proteins located on the cell surface. These receptors, like enzymes, have specific binding sites to which only a narrow range of structurally similar chemical substrates can bind. It is the change in the number of bound receptors over time that provides information to the cell regarding chemical gradients (Macnab and Koshland, 1972). In the presence of a gradient in an attractant (a chemical species to which bacteria favorably respond, such as a nutrient), bacteria are able to bias their random walk by decreasing their tumbling frequency when moving toward higher attractant concentrations thus extending the run lengths in that direction. This results in a net bias of movement toward more favorable conditions and is known as chemotaxis. It is important to note that experimental evidence suggests that this is the *only* mechanism by which chemotactic bacteria respond to an attractant. For example, the turn angle distribution is unaffected by the presence of an attractant (Macnab, 1980).

A cell balance equation for bacteria responding to one-dimensional gradients was derived by Ford and Cummings (1992) from Alt's general three-dimensional balance equations (Alt, 1980) which are based on Berg's physical picture of bacterial motion. This balance equation for one-dimensional gradients can be contrasted with the equations appropriate to motion of bacteria in one dimension used by Ford and coworkers (Ford et al., 1991; Ford and Lauffenburger, 1991) to analyze experimental data from the stopped flow diffusion chamber assay.

In this article, we apply a finite-element method to numerically solve the balance equation derived by Ford and Cummings (1992) for conditions relevant to experimental studies (Ford et al., 1991; Ford and Lauffenburger, 1991) which involve only one-dimensional attractant gradients. We then compare solutions of this balance equation to those obtained using a phenomenological one-dimensional model (Rivero et al., 1989) and to simulations of populations of individual bacteria (Frymier et al., 1993). The finite-element solution is then used to probe the effects on the bacterial migration of two different models of how bacteria respond when moving against an attractant gradient. Our results show that the two models for down-gradient behavior give significantly different solutions. In addition, we numerically evaluate the importance of a commonly neglected temporal derivative term in the relationship between the attractant gradient and the tumbling probability. Finally, we study the impact of each of these alternatives—the choice of balance equation, the model for down-gradient swimming behavior, and the neglect of the temporal derivative—on the experimentally measured transport coefficient for chemotaxis.

Balance Equations

In this Section, we briefly describe the balance equation for one-dimensional gradients derived by Ford and Cummings. This balance equation is a simplification of the full three-dimensional cell balance equation of Alt (1980) for bacteria moving in three dimensions subject to one-dimensional attractant gradients. We also describe the simpler phenomenological one-dimensional balance equations developed by Rivero et al. in order to contrast the two models.

Balance equation for one-dimensional attractant gradient

In Alt's three-dimensional cell balance equation (Alt, 1980), the cells are assumed to have piecewise linear paths (runs) where the mean speed v depends on position and time, that is, $v = v(\vec{r}, t)$. The probability per unit time that a cell moving in direction $\hat{s}$ at $\vec{r}$ at time t with run time τ (counted from the beginning of the run) tumbles at $\vec{r}$ at time t is given by $\beta(\vec{r}, \hat{s}, \tau, t)$. If a cell tumbles at $\vec{r}$ at time t after a run with direction $\hat{s}_1$, the probability that after tumbling it chooses the direction $\hat{s}_2$ as its new direction is $k(\vec{r}, \hat{s}_1, t; \hat{s}_2)$. We shall refer to k as the direction change probability distribution. The change in direction following a tumble is assumed to be the only mechanism for a cell changing direction, thus implying that cells are at sufficiently low density that collisions can be ignored. Alt's equation is then:

$$\frac{\partial \sigma(\vec{r}, \hat{s}, \tau, t)}{\partial t} = -\frac{\partial \sigma(\vec{r}, \hat{s}, \tau, t)}{\partial \tau} - \hat{s} \cdot \vec{\nabla}_{\vec{r}}[v(\vec{r}, t)\sigma(\vec{r}, \hat{s}, \tau, t)] - \beta(\vec{r}, \hat{s}, \tau, t)\sigma(\vec{r}, \hat{s}, \tau, t) \quad (1)$$

for $\tau > 0$ and

$$\sigma(\vec{r}, \hat{s}, 0, t) = \int_0^\infty \int \beta(\vec{r}, \hat{s}', \tau, t)\sigma(\vec{r}, \hat{s}', \tau, t)k(\vec{r}, \hat{s}', t; \hat{s})d\hat{s}'\,d\tau \quad (2)$$

for $\tau = 0$. Physically, Eq. 1 states that the rate of change in the population of cells at $\vec{r}$ at time t moving in direction $\hat{s}$ with run time τ is given by a term which takes into account the change in the run time of the cell population, a convective term which accounts for the net motion of the cells away from the point $\vec{r}$ and a loss term due to cells tumbling (with probability β, so density $\beta\sigma$). The subscript $\vec{r}$ on the divergence operator is meant to emphasize that the divergence is with respect to the spatial coordinate $\vec{r}$. Equation 2 states that the way in which one obtains an initial (that is, run time $\tau = 0$) population of cells moving in direction $\hat{s}$ is by considering cell populations which were moving in another direction $\hat{s}'$ and tumbled at time t with run time τ, $\beta(\vec{r}, \hat{s}', \tau, t)\sigma(\vec{r}, \hat{s}', \tau, t)$. This quantity is multiplied by the probability that the cell, after tumbling, moves in the direction $\hat{s}$, given by $k(\vec{r}, \hat{s}', t; \hat{s})$. One needs to add up over all such populations—hence, the integration over all directions $\hat{s}'$ and all run times τ. This general relationship applies to bacteria moving in three dimensions and is valid in the presence of multidimensional attractant

gradients. Note that in this expression the velocity is still assumed to be a function of time and position and that the tumbling probability is a function of position, direction, run time, and time. This general expression would be difficult to solve numerically for two reasons. First, the experimentally determined three-dimensional direction change probabililty distribution would have to be tabulated for a sufficient number of all the possible directions $\hat{s}$ and $\hat{s}'$ so that interpolations could be done with sufficient accuracy. In addition, there would be six independent variables in the full three-dimensional problem making this is a very computationally intensive problem to solve.

The full three-dimensional equation was simplified for the migration of bacteria in response to one-dimensional gradients of chemical attractants by Ford and Cummings (1992). The resulting cell balance equation is:

$$\frac{\partial n_z(z,\theta,t)}{\partial t} = -s_z \frac{\partial v(z,t) n_z(z,\theta,t)}{\partial z} - \beta(z,\theta,t) n_z(z,\theta,t) + \int_0^{\pi} \beta(z,\theta',t) n_z(z,\theta',t) K(\theta',\theta) \sin\theta' d\theta' \quad (3)$$

where $K(\theta', \theta)$ is the probability per unit angular measurement that a bacterium moving the direction θ' will change its direction to θ after tumbling. Equation 3 states that the time rate of change in the number density of bacteria at position z moving in the direction θ with respect to the z-axis (see Figure 11 in the Appendix) at time t is given by the sum of two loss terms (taking into account loss through convective motion away from the point z and through tumbling with probability density $\beta(z, \theta, t)$) and a gain term (taking into account bacteria which were moving in another direction θ' before tumbling and then moving in the direction θ).

The bacterial density that would be measured in an experiment is the angle independent density, $c(z, t)$, and is related to the angle dependent density, $n_z(z, \theta, t)$ by:

$$c(z,t) = \int_0^{\pi} n_z(z,\theta,t) \sin\theta d\theta \quad (4)$$

Equation 3 involves only three independent variables (z, θ and t) and requires as input the angle change distribution which is a function only of the two angles θ and θ'. In order to solve the cell balance equation, the functional form of the tumbling probability, β, must be specified. As noted previously, the tumbling probability is a function of the attractant gradient (∇a, where a is the concentration of the attractant) and the direction in which the bacterium is swimming. Macnab and Koshland (1972) presented experimental evidence that a bacterium senses the changing *spatial* concentration of an attractant during the running phase of its motion essentially by sensing the *temporal* change in concentration as it moves through the medium. Brown and Berg (1974) found that the run length of a bacterium moving in a direction that results in perception of a gradient increasing with time ($da/dt > 0$) is an exponential function of the perceived gradient. This observation was expressed mathematically in the form:

$$\ln \frac{\langle \tau \rangle}{\langle \tau_0 \rangle} = \nu \frac{dN_b}{dt}$$

where ν is a proportionality constant describing the fractional change in mean run time per unit time rate of change in cell surface receptors that are bound to attractant molecules and dN_b/dt is the time derivative of the number of bound receptors. To take into account the combined effects of spatial and temporal gradients, Rivero et al. (1989) proposed using this equation in the form:

$$\ln \frac{\langle \tau \rangle}{\langle \tau_0 \rangle} = \nu \frac{DN_b}{Dt} \quad (5)$$

where DN_b/Dt is the material derivative of the number of bound receptors:

$$\frac{DN_b}{Dt} = \frac{\partial N_b}{\partial t} + v\hat{s}\cdot\nabla N_b = \frac{dN_b}{da}\frac{\partial a}{\partial t} + v\hat{s}\cdot\nabla a \frac{dN_b}{da} \quad (6)$$

In the model of Rivero et al. (1989) (hereafter denoted the RTBL model), it was assumed that $\partial a/\partial t \ll v\hat{s}\cdot\nabla a$, yielding:

$$\frac{DN_b}{Dt} \approx v\hat{s}\cdot\nabla a \frac{dN_b}{da} \quad (7)$$

For a single population of homogeneous receptors, Rivero et al. assume the following form for the dependence of the change in the number of bound receptors on the attractant concentration:

$$\frac{dN_b}{da} = \frac{N_T K_d}{(K_d + a)^2} \quad (8)$$

where K_d is the dissociation constant for the attractant-receptor binding and N_T is the total number of receptors. Substituting Eqs. 7 and 8 into Eq. 5 gives:

$$\ln \frac{\langle \tau \rangle}{\langle \tau_0 \rangle} = \nu v \frac{N_T K_d}{(K_d + a)^2} \hat{s}\cdot\nabla a \quad (9)$$

Rivero et al. define a chemotactic sensitivity coefficient, χ_0, as:

$$\chi_0^{3D} = \nu v^2 N_T \quad (10)$$

where superscript 3D indicates explicitly that this is the definition for motion in three dimensions. Using the definition of χ_0^{3D}, Eq. 10, we can write Eq. 9 as:

$$\ln \frac{\langle \tau \rangle}{\langle \tau_0 \rangle} = \frac{\chi_0^{3D}}{v} \frac{K_d}{(K_d + a)^2} \hat{s}\cdot\nabla a \quad (11)$$

For a Poisson process, the probability of tumbling $\beta(\vec{r}, \hat{s}, t)$ is given by:

$$\beta(\vec{r}, \hat{s}, \tau, t) = \frac{1}{\langle \tau \rangle} = \beta_0 \exp\left[-\frac{\chi_0^{3D}}{v} \frac{K_d}{(K_d + a)^2} \hat{s}\cdot\nabla a \right] \quad (12)$$

For the special case of a one-dimensional attractant gradient in the z-direction, $\hat{s}\cdot\nabla a$ reduces to $(\partial a/\partial z)\cos\theta$ and $\beta(\vec{r}, \hat{s}, \tau, t) = \beta(z, \theta, t)$. Depending on the swimming behavior of the

particular bacterial species, an alternate form of Eq. 12 may be appropriate which is given by:

$$\beta(z, \theta, t) = \begin{cases} \beta_0 exp(-\epsilon), & \epsilon > 0 \\ \beta_0, & \epsilon < 0 \end{cases} \tag{13}$$

where

$$\epsilon = \frac{\chi_0^{3D}}{v} \frac{K_d}{(K_d+a)^2} \hat{s} \cdot \nabla a = \frac{\chi_0^{3D}}{v} \frac{K_d}{(K_d+a)^2} \frac{\partial a}{\partial z} \cos\theta$$

That is, for some bacterial species the probability of tumbling does not increase when the bacteria are moving in the direction of a decreasing attractant gradient but simply returns to β_0, the basal tumbling frequency in the absence of a gradient (Berg and Brown, 1972).

One-dimensional RTBL model

Segel (1977) and Rivero et al. (1989) have developed simpler phenomenological models based on individual cell motion in one direction only. The one-dimensional balance equations of Segel are:

$$\frac{\partial n^+}{\partial t} = -\frac{\partial}{\partial z}(sn^+) + p^- n^- - p^+ n^+ \tag{14}$$

$$\frac{\partial n^-}{\partial t} = \frac{\partial}{\partial z}(sn^-) + p^+ n^+ - p^- n^- \tag{15}$$

where $n^+(z, t)$ is the density of cells at point z at time t moving in the positive z direction and $n^-(z, t)$ is the density of cells at point z at time t moving in the negative z direction, s is the one-dimensional, scalar swimming speed of the bacteria, $p^+ = p^+(z, t)$ is the probability per unit time that a cell moving in the positive z direction tumbles and becomes a cell moving in the negative z direction, and $p^- = p^{-1}(z, t)$ is the probability per unit time that a cell moving in the negative z direction tumbles and becomes a cell moving in the positive z direction. Equation 14 states that the time rate of change in the number density of cells moving in the $+z$ direction is equal to the sum of the loss due to bacterial motion, the gain due to cells initially moving in the $-z$ direction tumbling and moving in the $+z$ direction, and the loss due to cells initially moving in the $+z$ direction tumbling and moving in the $-z$ direction. Similarly, Eq. 15 states that the time rate of change in the number density of cells moving in the $-z$ direction is equal to the sum of the loss due to bacterial motion, the gain due to cells initially moving in the $+z$ direction tumbling and moving in the $-z$ direction, and the loss due to cells initially moving in the $-z$ direction tumbling and moving in the $+z$ direction. Note that inherent in this development is the assumption that the bacteria are constrained to motion only in two directions, the $\pm z$ directions.

The assumption of a Poisson process for tumbling leads to:

$$\beta^{\pm} = \frac{1}{\langle \tau^{\pm} \rangle} \tag{16}$$

where $\beta^{\pm} = p_t^{\pm}(z, t)$ is the probability that a cell moving in the $\pm z$ direction tumbles and $\langle \tau^{\pm} \rangle$ is the mean run time for cells moving in the $\pm z$ directions, respectively. The analogous assumption to Eq. 12 is:

$$p^{\pm} = \beta^{\pm} p_r \tag{17}$$

where p_r is the probability that a cell reverses direction after tumbling and

$$\beta^{\pm} = \beta_0 \exp\left[\mp \frac{\chi_0^{1D}}{s} \frac{K_d}{(K_d+a)^2} \frac{\partial a}{\partial z} \right] \tag{18}$$

where β_0 is the basal tumbling frequency. As before, K_d is the dissociation constant for the attractant-receptor binding and χ_0^{1D} is the one-dimensional chemotactic sensitivity parameter. In the RTBL model, Eqs. 16–18 form a set of constitutive equations for Segel's cell balance equations.

Methodologies

In this section, we describe the details of the finite-element method (FEM) applied to the solution of the balance equation for a one-dimensional attractant gradient. We also briefly review the experimental assay (whose function is modeled here using the finite-element and cellular dynamics methods) and the cellular dynamics (CD) simulation methodology.

Finite-element method solution

The numerical solutions of the balance equation for one-dimensional attractant gradients, Eq. 3, presented here utilized Galerkin's method on finite elements (Allaire, 1985) for integration over the spatial variables z and θ. Equation 3 represents an unusual application of the finite-element technique because it is an integro-partial differential equation, in contrast to the typical application to purely partial differential equations. A weighted implicit/explicit finite-difference method was used for the integration over time. With the definition:

$$F(z, \theta, t) = -s_z \frac{\partial v(z, t) n_z(z, \theta, t)}{\partial z} - \beta(z, \theta, t) n_z(z, \theta, t) + \int_0^{\pi} \beta(z, \theta', t) n_z(z, \theta', t) K(\theta', \theta) \sin\theta' d\theta' \tag{19}$$

and first-order differencing in time, Eq. 3 gives:

$$\frac{n_z(z, \theta, t_m) - n_z(z, \theta, t_{m-1})}{\Delta t} = \omega F_m + (1-\omega) F_{m-1} \tag{20}$$

where the subscript m indicates that F is evaluated at the current time step ($t = t_m = t_0 + m\Delta t$) and the subscript $m-1$ indicates that F is evaluated at the previous time step. The weighting parameter ω can be varied from 1 (resulting in a fully implicit method) to 0 (resulting in a fully explicit method). The $z-\theta$ space was divided into finite rectangular elements, as shown in Figure 1. The initial conditions used in the solutions presented in this work correspond to those of the stopped flow diffusion chamber (SFDC) assay of Ford and co-workers (see the description of the stopped flow diffusion chamber in the following section). An initial uniform bacterial density and an initial step gradient of an attractant are assumed, that is,

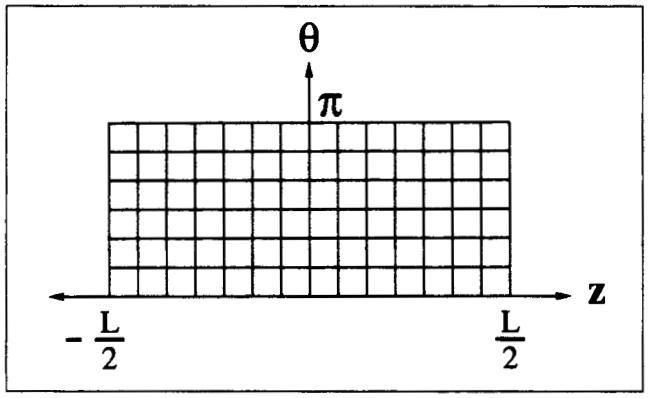

Figure 1. Example of the type of grid used in obtaining the finite-element solutions.

Actual grids used contained 200 divisions in the z direction and ten divisions in the θ direction. Length L was 1.2 cm.

$$n_z(z, \theta, t=0) = n_{z0}, \quad -L/2 \le z \le L/2, \quad 0 \le \theta \le \pi \tag{21}$$

and

$$a(z, t=0) = 0, \quad -L/2 \le z < 0,$$

$$a(z, t=0) = a_0, \quad 0 < z \le L/2,$$

$$a(z, t) = \frac{a_0}{2}\left[1 + \operatorname{erf}\left(\frac{z}{\sqrt{4Dt}}\right)\right], \quad t > 0, \ -L/2 \le z \le L/2. \tag{22}$$

where a_0 is the initial attractant concentration introduced into one half of the chamber, D is the diffusion coefficient of the attractant, z is the position along the z axis, and t is time. The time-dependent solution given above for the attractant concentration profile can be found in Crank (1979).

A bilinear function was used to approximate $n_z(z, \theta, t)$ on the elements, that is,

$$n_z(z, \theta, t)^{(e)} = \gamma_1^{(e)} + \gamma_2^{(e)} z + \gamma_3^{(e)} \theta + \gamma_4^{(e)} z\theta \tag{23}$$

where the superscript (e) denotes the element e. The constants γ_1, γ_2, γ_3, and γ_4 are related to the (unknown) nodal values of the dependent variable $n_z(z, \theta, t)$. The interpolation function for $n_z(z, \theta, t)$ can also be approximated by the more convenient form:

$$n_z(z, \theta, t)^{(e)} = G_i n_{z(i)} + G_j n_{z(j)} + G_k n_{z(k)} + G_l n_{z(l)} \tag{24}$$

where the constants $n_{z(i)}$, $n_{z(j)}$, $n_{z(k)}$, and $n_{z(l)}$ are the values of $n_z(z, \theta, t)$ at the "nodes" of the element e (see Figure 2) and G_i, G_j, G_k, and G_l are called the shape functions of e and are related to γ_1, γ_2, γ_3, and γ_4. The shape functions are constructed so that $n_z(z, \theta, t)$ varies linearly along the sides of the element and takes on its nodal values at the nodes i, j, k, and l.

The integration over θ' indicated in Eq. 3 was calculated using a two-point Gaussian integration on each element. Due to the small variation of the integrand over the width of an element in θ-space ($\pi/10$), a two-point Gaussian was found to be sufficiently accurate; higher-order Gaussian quadratures did not lead to significantly more accurate results. The values of

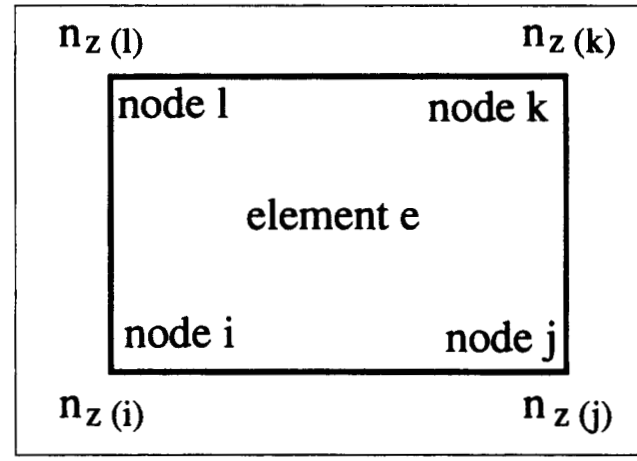

Figure 2. Example of a single element in the grid.

"Nodes" of the grid are the corners of the elements. Values of dependent variable $n_z(z, \theta, t)$ at the nodes are $n_{z(i)}$, $n_{z(j)}$, $n_{z(k)}$, and $n_{z(l)}$.

θ and θ' for which the direction change is needed are therefore known at the beginning of the solution method permitting $K(\theta', \theta)$ to be calculated at the outset of the solution procedure and tabulated so that it need not be recalculated at each time step (see the Appendix). The solutions to the balance equation presented here were obtained using a grid of 2,000 elements in the $z-\theta$ space. A typical finite-element solution to the balance equation for one-dimensional attractant gradients requires about 40 CPU min on an IBM RS/6000 Powerstation 320.

Stopped flow diffusion chamber assay

The stopped flow diffusion chamber (SFDC) assay was developed by Ford and co-workers (Ford et al., 1991) to permit measurement of the two bacterial transport properties, the random motility coefficient, μ_0, and the chemotactic sensitivity coefficient, χ_0. In the absence of an attractant gradient, the random motility coefficient can be expressed in terms of the cellular quantities cell speed v and mean run time $\langle\tau\rangle$ (Lovely and Dalquist, 1975):

$$\mu_0 = \frac{v^2\langle\tau\rangle}{3(1-\psi)} \tag{25}$$

where ψ is the average value of $\cos(\alpha)$, α being the angle between the direction vectors of a cell before and after tumbling. This is a general result for three-dimensional motion of bacteria assuming only a constant swimming speed, straight line swimming between tumbles, and a Poisson distribution for run lengths. The random motility coefficient is analogous to the diffusion coefficient in Fickian diffusion, and in fact one can show at the macroscopic level that the diffusive part of the bacterial flux, J_b^{diff}, is given by (Keller and Segel, 1971; Rivero et al., 1989):

$$J_b^{\text{diff}} = -\mu_0 \nabla c(\vec{r}, t) \tag{26}$$

where $c(\vec{r}, t) = \int n(\vec{r}, \hat{s}, t) d\hat{s}$ is the bacterial density.

The SFDC is shown schematically in Figure 3. For assays

of chemotactic bacteria in the SFDC, a suspension of bacteria at concentration c_0 is pumped at a uniform rate into the upper port of the chamber and a mixture of attractant at concentration a_0 and bacteria at concentration c_0 is pumped at a uniform rate into the lower port. Fluid exits through ports at the centerline of the chamber, and the flow rates are controlled by a dual piston syringe pump so that for times $t<0$, the two impinging streams form a step change in the attractant concentration at the center of the chamber. At time $t=0$, flow into and out of the SFDC is stopped and the attractant begins to diffuse into the upper half of the chamber generating a time-dependent gradient. As bacteria sense the gradient, a band of high cell density forms where the gradient is large and moves downward in the chamber to regions of higher attractant concentration. The experimental geometry is one of symmetry in two dimensions (the x and y directions in Figure 3) with an attractant gradient in the third dimension (the z direction). The bacterial density profile in the SFDC is measured using light scattering and is analyzed to determine the value of the chemotactic sensitivity coefficient. An independent experiment in the absence of the gradient, in which one side of the chamber is initialized with no bacteria present, is used to measure μ_0. For details, refer to the original work by Ford et al. (1991) and Ford and Lauffenburger (1991).

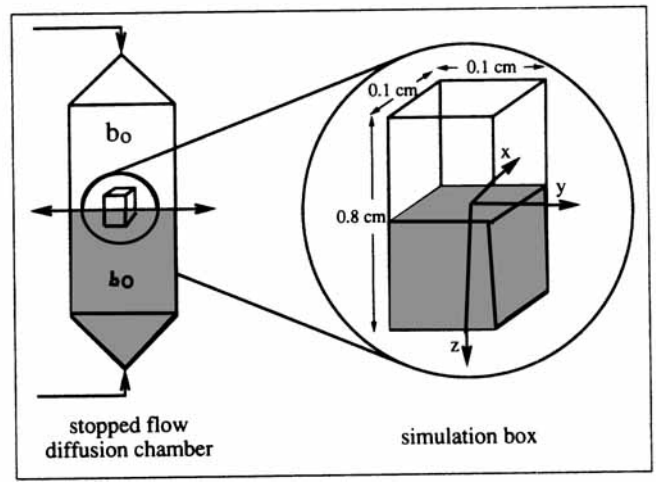

Figure 3. Representation (left) of the SFDC used by Ford and coworkers.

Impinging flow from the upper and lower ports creates an initial step change in attractant gradient at the center of the chamber and a uniform distribution of bacteria. Approximate dimensions of the chamber are 4 cm. × 2 cm. × 0.2 cm. On the right is an exploded view of the simulation box which is referred to later in the text.

Cellular dynamics simulations

Cellular dynamics (CD) simulation methodology was developed by us as a method for studying the collective transport properties of populations of bacteria essentially by simulating the dynamics of large populations of individual bacteria (Frymier et al., 1993). It thus shares considerable common philosophical ground with molecular dynamics simulations methods used to predict the many-body thermophysical properties of liquids (Allen and Tildesly, 1987). In essence, the stochastic differential equation which describes the dynamics of an individual bacterium is solved for 10^4–10^5 bacteria in a geometry appropriate to a small subvolume (1 mm × 1 mm × 8 mm) of the SFDC located at its center with the long axis parallel to the coordinated direction (z) in which there is an attractant gradient. Periodic boundary conditions are used at the two faces perpendicular to the z axis since the bacterial density is observed experimentally to have remained at the uniform initial value at these distances from the center of the SFDC during the course of a typical experiment (6–12 min).

The stochastic differential equation solved in the CD simulation embodies the same individual cell dynamics as are assumed in Alt's equations and the general balance equation for one-dimensional gradients, Eq. 3. Hence, from the mathematical point of view, the density profiles obtained from the CD simulations should be the same as those obtained from the FEM solution provided the same boundary conditions (that is, SFDC geometry), operating conditions and sensing mechanisms are used in both cases. [This equivalence is exactly the same as that between Brownian dynamics simulations of kinetic theory models of polymeric molecules at infinite dilution and the corresponding "diffusion equation" solutions for the phase space density (Bird and Öttinger, 1992).] The advantage of the FEM solution to Eq. 3 over CD simulation is that the numerical computation involved is considerably less. This is because the error in CD simulations is $O(N^{-1/2})$ while the computation time is $O(N)$, where N is the number of bacteria simulated. Obtaining results from CD simulation with errors similar to those of FEM (around 1%) would be computationally expensive. For example, with 20,000 bacteria the noise in CD appears to be around 5%, so reducing this to 1% would require 25 times this number (or 500,000) bacteria and would require 26 h of CPU time on an IBM RS/6000 Powerstation 320 for a simulation corresponding to 6 min of real time. The advantage of the CD method is that it permits visualization of the individual bacterial motion as well as the collective motion of the population.

Results

In this section, we present the results of the numerical solution of the balance equation for one-dimensional attractant gradients, Eq. 3, using the finite-element method (FEM) discussed in the previous section, and compare them to the RTBL model and CD simulation results.

Before doing so, it is instructive to summarize the relationship between the three approaches being used to describe bacterial migration in this article, RTBL, the FEM solution to the balance equation for one-dimensional attractant gradients, and CD simulations. All three approaches have the same conceptual basis: that tumbling in bacteria is governed by a stochastic Poisson process and is related to the attractant gradient by the experimentally derived relationship Eq. 12. The CD simulation method is, in essence, a brute force Monte Carlo method for solving Alt's equations, Eqs. 1 and 2. The FEM solution is for the reduced form of Alt's equations derived by Ford and Cummings (1992) for the case of a one-dimensional attractant gradient by exploiting symmetry in two of three coordinate directions. Thus, CD and FEM are alternative methods for solving the same model—that is, the same equations for the same physical situation—and thus should yield equivalent results. Note that the CD method involves the solution of the dynamical equations for individual cells and thus, unlike the

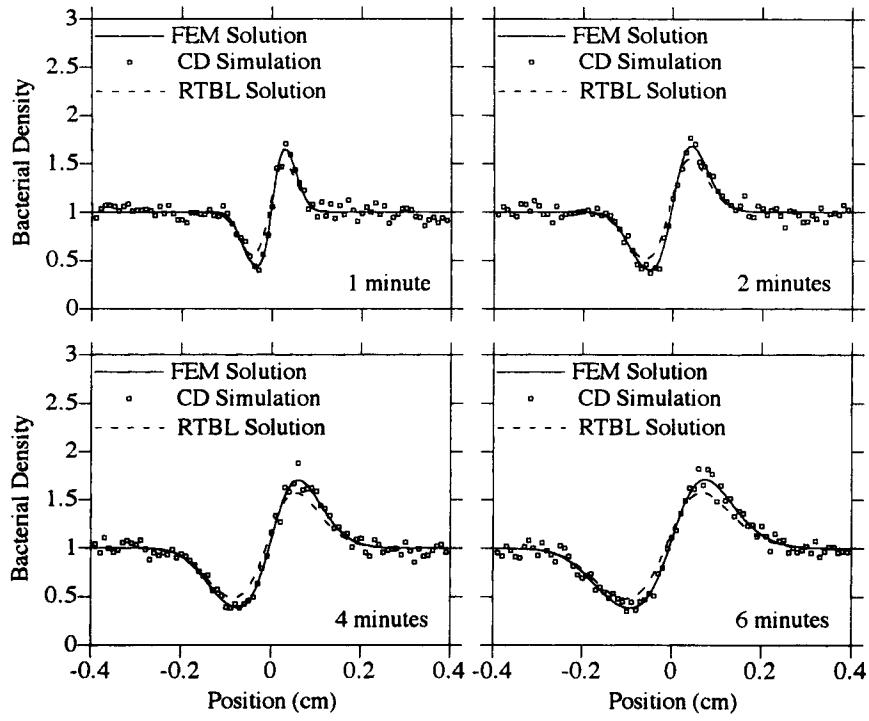

Figure 4. Comparison of the finite-element solution of the balance equation for one-dimensional gradients: Eq. 3 (—), CD simulation (□), and RTBL model (· · · ·) for $\chi_0^{3D} = 3.5 \times 10^{-4}$ cm²/s.

Dimensionless bacterial density, c/c_0 is plotted as a function of the position z along the SFDC for times of 1, 2, 4, and 6 min. Position $z = 0$ corresponds to the position of the initial step change in the attractant concentration at $t = 0$ with a fucose concentration of 0.2 mM initially in the bottom of the SFDC ($0 < z \leq 0.4$ cm in the graphs).

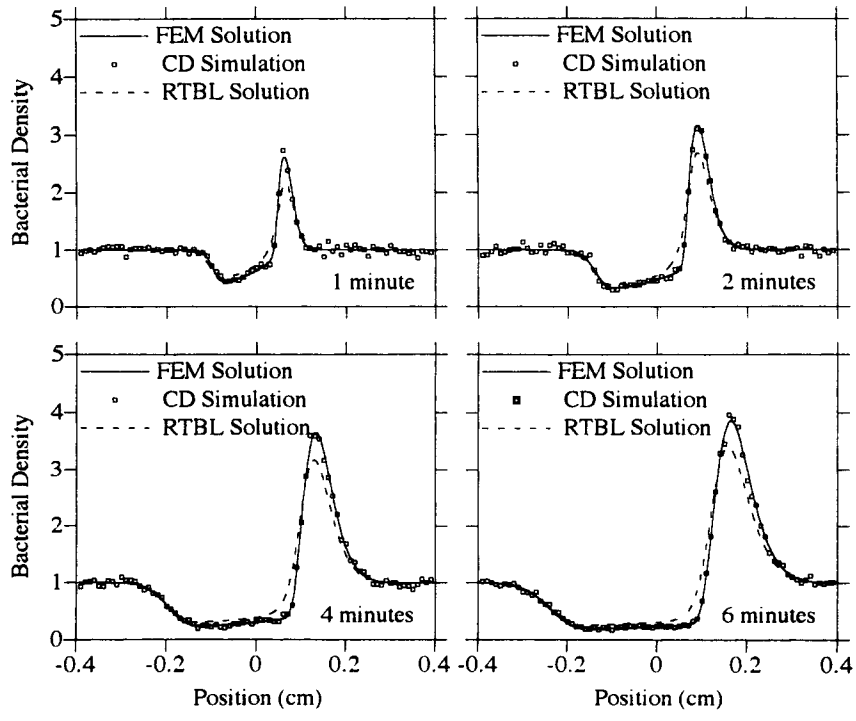

Figure 5. Comparison of the finite-element solution of the balance equation for one-dimensional gradients: Eq. 3 (—), CD simulation (□), and RTBL model (· · · ·) for $\chi_0^{3D} = 105 \times 10^{-4}$ cm²/s.

Solutions are shown at 1, 2, 4, and 6 min.

FEM solution, is unable to take advantage of the overall symmetry of the population as it responds to a one-dimensional attractant gradient. This is one sense in which the FEM solution is more efficient. By contrast to the model underlying the CD simulation and the FEM solution, the RTBL model involves an additional physical assumption, namely that the bacteria are confined to one dimension in their motion (Ford and Cummings, 1992).

We compare the FEM solution to that obtained by CD simulations and to that obtained from the RTBL model for two of the cases we studied in a previous article (Frymier et al., 1993) which contained CD simulations of *E. coli* in the presence of a gradient in fucose. We consider for comparison both the bacterial density profiles and the resulting bacterial transport coefficient for chemotaxis. We then consider variations on the cell sensory mechanism beyond those previously studied using either CD simulation or RTBL and compare FEM solutions to experimental data for the response of *E. coli* bacteria to a gradient of α-methylaspartate.

Comparison between models

We begin with a comparison of FEM, CD, and RTBL for the set of conditions shown in Table 1 and $\chi_0^{3D} = 3.5 \times 10^{-4}$ cm^2/s (equivalent to $\chi_0^{1D} = 0.88 \times 10^{-4}$ cm^2/s). Note that the RTBL quantities for cell speed (v) and chemotactic sensitivity coefficient χ_0 in Table 1 are one-dimensional quantities and are related to the corresponding three-dimensional quantities used in the CD and FEM calculations according to the relationship derived by Ford and Cummings (1992):

$$v^{3D} = 2v^{1D} \tag{27}$$

which leads to the following relationship between χ_0^{1D} and χ_0^{3D} (Frymier et al., 1993):

$$\chi_0^{3D} = 4\chi_0^{1D} \tag{28}$$

These relationships were verified by Frymier et al. as being essential to obtain consistency between the one-dimensional RTBL and three-dimensional descriptions. The attractant concentration, diffusivity, and dissociation constant (a_0, D, and K_d) and bacterial properties (β_0, v, and p_r) in Table 1 correspond to those in SFDC experiments measuring the response of *E. coli* bacteria to a gradient of fucose reported by Ford et al. (1991). The value $\chi_0^{3D} = 3.5 \times 10^{-4}$ cm^2/s corresponds to the experimentally measured value for this system. The value of $\chi_0^{3D} = 105 \times 10^{-4}$ cm^2/s is high, but is consistent with values measured experimentally for bacteria cultured in limited nutrient conditions (Mercer et al., 1993).

In Figures 4 and 5, the FEM solution of Eq. 3 is compared to the CD simulation and to the solution of the RTBL model for the conditions given in Table 1 with $\chi_0^{3D} = 3.5 \times 10^{-4}$ cm^2/s over a period corresponding to six minutes of elapsed time. The bacterial density $c(x, t)$ given by Eq. 4 is plotted in dimensionless form as a function of position. The dimensionless bacterial density is defined as c/c_0 where $c_0 = 2n_{z,0}$ is the initial uniform bacterial density.

The model for the tumbling probability used in the FEM solution and the CD simulations is Eq. 12 and in the RTBL model is Eq. 18. This is consistent with the model used in previously reported numerical studies (Ford et al., 1991; Frymier et al., 1993). The first observation is that the FEM solution is completely consistent with the CD simulation as expected on the basis of the equivalence of the models. Second, it is clear that there is a small but discernible, quantitative difference between the predictions of the RTBL model and the solution of the three-dimensional models (FEM and CD). In our previous comparison between CD and RTBL (Frymier et al., 1993), the level of noise in the CD simulations had made it difficult to assert with a high degree of certainty that there were differences between the predictions of RTBL and of models (such as CD and Eq. 3) which take into account the full three-dimensional character of the bacterial motion. These differences are clearly evident in both Figures 4 and 5, with the RTBL model having a lower peak and a more shallow trough than the three-dimensional models.

The computation times for the FEM solution, CD simulation (using 20,000 bacteria) and the RTBL model (solved by finite differences) are 39, 63, and 1 min, respectively, of CPU time on an IBM RS/6000 Powerstation 320.

Effect of model selection on the chemotaxis transport coefficient

An important question is to what extent the difference between the RTBL and FEM solutions results in significant differences in the transport properties which would be inferred by comparison with experiment. In particular, the value of χ_0 is obtained experimentally by measuring $N(t)$, the number of bacteria entering the upper chamber of the SFDC as a function of time t. For RTBL, it is known that $N(t) \propto t^{1/2}$ with a slope that increases monotonically with χ_0 (Staffeld and Quinn, 1989). Experimentally, it is also found that $N(t) \propto t^{1/2}$, so the value of χ_0 inferred from the experimental data is determined by applying the mathematical model to the conditions of the experiment; the inferred value of χ_0 from the experiment is that which yields the same theoretical slope of $N(t)$ vs. $t^{1/2}$ as that given by a linear least-squares regression of the experimental data. We illustrate this method explicitly using the experimental data shown in Figure 6 which contains a plot of $N(t)$ vs. $t^{1/2}$ for *E. coli* responding to α-methylaspartate in the SFDC (Strauss, 1992). The least-squares fitted slope in Figure 6 has an error of 4.7% calculated from the standard deviation based on its relationship to the R^2 correlation coefficient of 0.991 obtained from the linear regression analysis (Milton and Arnold, 1990). For χ_0 in the range of our experimental data, χ_0 and the slope in the experimental $N(t)$ vs. $t^{1/2}$ plot are linearly related, so that when the value of χ_0 is found which yields a slope for the area vs. $t^{1/2}$ curve equal to the experimental value (in this case, $\chi_0 = 1.9 \times 10^{-4}$ cm^2/s), we assume that the only source of error in χ_0 is the experimentally determined slope. This linear relationship implies that χ_0 and the slope have the same fractional error. From this we conclude that the error in χ_0 is approximately 5%.

Since the RTBL model has been shown to be a small gradient approximation of Eq. 3, one can probe the error in χ_0 that might result from the use of RTBL rather than Eq. 3 by fitting the $N(t)$ vs. $t^{1/2}$ from RTBL to the corresponding result for Eq. 3 and then comparing the inferred value of χ_0^{1D} to the value obtained using the balance equation for one-dimensional attractant gradients, Eq. 3. For $\chi_0^{3D} = 3.5 \times 10^{-4}$ cm^2/s, we solve Eq. 3 by FEM and fit RTBL to the resulting $N(t)$ vs. $t^{1/2}$ plot

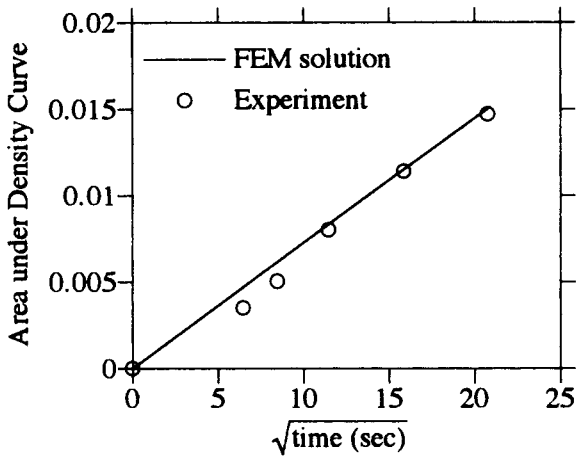

Figure 6. Area between the dimensionless bacterial density curve and $c/c_0 = 1$ in the half of the SFDC with a high concentration of attractant plotted as a function of $t^{1/2}$ for the case in Figure 8.

Value of χ_0 used to produce the model results is $\chi_0^{3D} = 1.9 \times 10^{-4}$ cm^2/s and yields the same slope as a linear least-squares regression of the experimental data. In this comparison, the offset time has been included in the simulation solutions (Staffeld and Quinn, 1989).

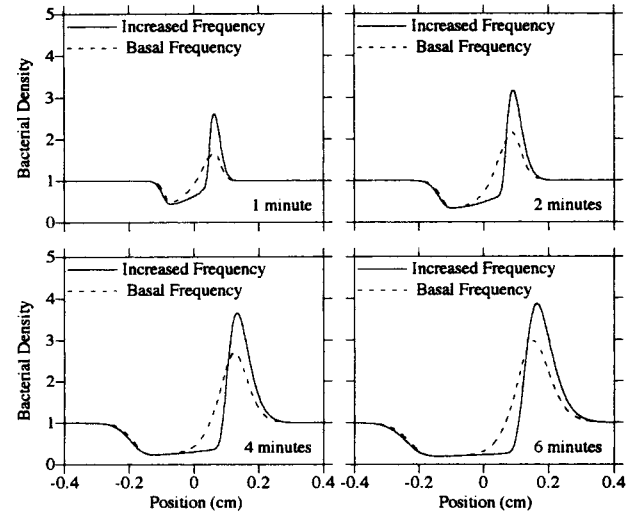

Figure 7. Finite-element solutions to the balance equation for one-dimensional gradients for $\chi_0^{3D} = 105 \times 10^{-4}$ cm^2/s.

In the first case (—), the tumbling frequency β is allowed to increase above its basal level β_0 for populations of bacteria moving against the attractant gradient according to Eq. 12. In the second case (- - - -), the tumbling frequency is assumed to return to its basal value for bacteria moving against an attactant gradient according to Eq. 13.

and find that the best fit is given by $\chi_0^{1D} = 1.2 \times 10^{-4}$ cm^2/s which is 31% higher than the expected value of $\chi_0^{3D}/4 = 0.88 \times 10^{-4}$ cm^2/s. For $\chi_0^{3D} = 105 \times 10^{-4}$ cm^2/s, the best fit of RTBL to the $N(t)$ vs. $t^{1/2}$ plot is given by $\chi_0^{1D} = 88.0 \times 10^{-4}$ cm^2/s which is 230% higher than the value of 26.0×10^{-4} cm^2/s used in the FEM calculation. These two examples are consistent with many other calculations we have performed in which we have found that the value of χ_0 required by RTBL to fit the FEM solution is higher than the value of χ_0 used in the FEM solution. This observation suggests that the values of χ_0 inferred by fitting RTBL calculations to experimental measurements are likely to be overestimates, although the physical basis for this discrepancy is not obvious.

Having established the correctness of the FEM solution to Eq. 3 by comparison to CD simulation, it is clear that the FEM solution provides a convenient and computationally inexpensive route to calculating the bacterial migration profiles for bacteria subject to one-dimensional attractant gradients. It is thus the appropriate vehicle for comparison with experimental measurements, particularly for inferring values of transport coefficients, and in the second article in this series, the FEM solution is used to determine transport coefficients in systems subject to multiple gradients. In the remainder of this article, however, we will investigate two questions concerning the model for the tumbling probability.

The first question is: How do bacterial density profiles calculated using Eq. 13 for the tumbling probability (corresponding to bacteria returning to the basal tumbling frequency when moving away from an attractant) differ from those obtained using Eq. 12 (corresponding to bacteria increasing their tumbling frequency when moving away from an attractant), as has been assumed in previously published analyses (Ford and Lauffenburger, 1991)? This question has important bearing on the interpretation of bacterial density transport coefficients since it is known that *E. coli* obey Eq. 13 rather than Eq. 12 (Berg and Brown, 1972).

In Figure 7, we first compare the results for the two different tumbling probability models, Eqs. 12 and 13, using the Table 1 parameters in Eq. 3. It is clear that the difference in tumbling probability has a large effect on the bacterial density profile for these cases. Figure 7 shows that the solution obtained using Eq. 13 for the tumbling probability would result in lower numbers of bacteria moving into the half of the chamber where the attractant concentration is highest. Therefore, a higher value of χ_0^{3D} would be inferred by fitting solutions obtained using Eq. 13 to experimental data than would be inferred if Eq. 12 were used.

The value of χ_0^{3D} used in the solutions shown in Figure 7 is at the upper limit of values that one would expect to encounter experimentally (Mercer et al., 1993) and was chosen to emphasize the difference in solutions obtained using the two models for the tumbling probability. Next we consider the effect of the choice of tumbling probability models on the transport coefficient for chemotaxis by comparing FEM solutions to experimental data for *E. coli* responding to α-methylaspartate. The conditions at which the experiment was performed are given in Table 2 and are used in the subsequent model calculations.

Figure 8 compares the solution of the balance equation for one-dimensional gradients using Eq. 12 and Table 2 parameter values to the experimental data of Strauss (1992) for *E. coli* responding to an initial step gradient of α-methylaspartate in the SFDC.

The model solution shown in Figure 9 used Eq. 13 to calculate the tumbling probability. While the model solutions shown in Figures 8 and 9 are very similar, the value of χ_0^{3D} used to obtain the solution in Figure 9 represents a 100% increase over the value used to obtain the solution in Figure

Table 1. Constants Used in the CD Simulation and Solving Eq. 3 and the RTBL Equation for Comparisons Shown in Figures 4 and 5

Quantity	β_0 (s^{-1})	v (μm/s)	a_0 (mM)	$\chi_0 \times 10^4$ (cm^2/s)	$D \times 10^6$ (cm^2/s)	K_d (mM)	p_r
Eq. 3 and CD	0.17	22.0	0.2	3.5, 105	6.9	0.08	—
RTBL	0.17	11.0	0.2	0.88, 26.0	6.9	0.08	0.32

Table 2. Conditions for Experimental Measurement of the Response of *E. coli* to α-methylaspartate (Strauss, 1992)

Quantity	v (μm/s)	a_0 (mM)	$\mu_0 \times 10^7$ (cm^2/s)	$D \times 10^6$ (cm^2/s)	K_d (mM)
Value	22.0	0.01	8.8	7.1	0.125

8 which incorporated Eq. 12. Specifically, if we assume that the tumbling probability is given by Eq. 12 (which states that bacteria moving against the attractant gradient are capable of increasing their tumbling frequency above the basal level), then the value of χ_0 obtained by fitting to the experimental data is $\chi_0 = (1.9 \pm 0.1) \times 10^{-4}$ cm^2/s. If we assume that the tumbling probability is given by Eq. 13 (bacteria moving against the attractant gradient return to the basal tumbling frequency) and go through the fitting procedure described previously, we find $\chi_0 = (3.8 \pm 0.2) \times 10^{-4}$ cm^2/s. Therefore, determination of the chemotactic sensitivity (as reflected in χ_0) from experimental data requires *a priori* knowledge of whether Eq. 12 or 13 applies for the particular bacteria under investigation. We note that the 100% increase in χ_0^{3D} obtained using Eq. 13 rather than Eq. 12 is not a general result but is consistent with the small values of χ_0^{3D} involved. It can be shown that in the limit of small ϵ, in which case the exponentials in Eqs. 13 and 12 can be linearized, this factor of two naturally arises using the small ϵ perturbative expansion of Ford and Cummings (1992).

The second question is: To what extent is Eq. 7 a valid approximation for Eq. 6 for conditions such as those that exist in the SFDC? At very short times, because the attractant concentration in one half of the chamber is initially zero, it might be expected that the temporal derivative could be quite large, so that Eq. 7 might not be satisfied. In Figure 10, bacterial density profiles are shown both including and neglecting the temporal derivative, and it is clear that for times typically studied with the SFDC, there is no practical difference in the density profiles if the temporal derivative is included. Thus, it appears that the neglect of the temporal derivative is a valid assumption.

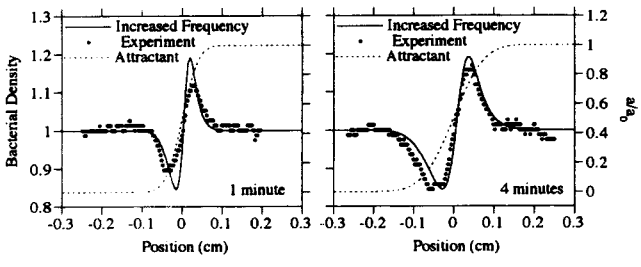

Figure 8. FEM solution to the balance equation for one-dimensional gradients (—) and experimental data (Strauss, 1992) (○) for the response of *E. coli* to α-methylaspartate in the SFDC with a 0.01 mM initial concentration of α-methylaspartate in the bottom of the SFDC (right side of figure).

Also shown (----) is the dimensionless attractant concentration, a/a_0. In the FEM model solution, the tumbling frequency β is allowed to increase above its basal level β_0 for populations of bacteria moving against the attractant gradient according to Eq. 12. The value of χ_0^{3D} used in the model solution was 1.9×10^{-4} cm^2/s.

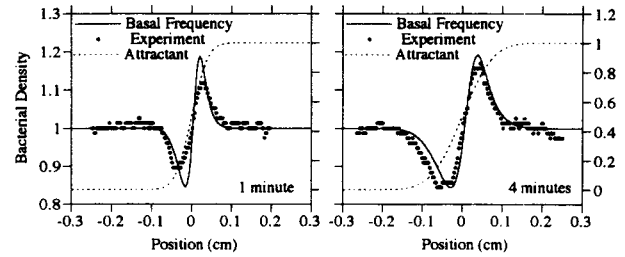

Figure 9. FEM solution to balance equation for one-dimensional gradients (—) and experimental data (Strauss, 1992) (○) for the response of *E. coli* to α-methylaspartate in the SFDC.

In the FEM model solution, the tumbling frequency β returns to its basal value β_0 for populations of bacteria moving against the attractant gradient according to Eq. 13. Value of χ_0^{3D} used in the model solution was 3.8×10^{-4} cm^2/s.

Conclusion

The reduced cell balance equation for one-dimensional attractant gradients derived by Ford and Cummings (1992) were solved in the context of the stopped flow diffusion chamber assay using a finite-element technique. The accuracy of the numerical solution was confirmed by comparison to cellular dynamics simulation which incorporated the same mechanistic

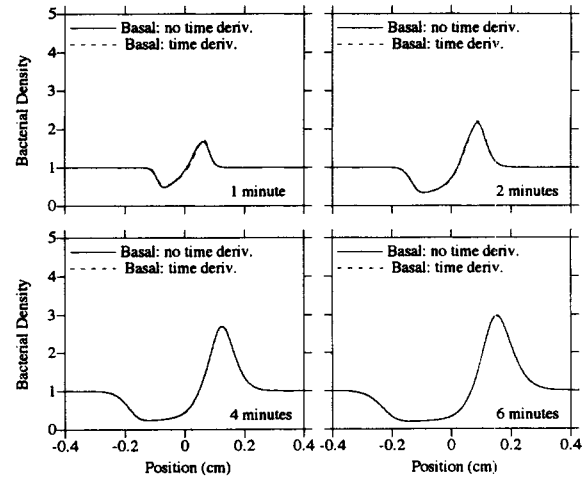

Figure 10. Finite-element solutions to the balance equation for one-dimensional gradients.

In the first case (—), the partial derivative with respect to time is included in the substantial derivative of the number of bound receptors (Eq. 6). In the second case (----), the partial derivative with respect to time is omitted (Eq. 7). Only a slight difference between the solutions is seen at 1 and 2 min and the two solutions are identical at 4 and 6 min on the scale of this graph. Both cases assume that the tumbling frequency returns to its basal value for cells moving in a direction against the attractant gradient.

Table 3. χ_0^{3D} Values Obtained from Fitting Model Solutions to Experimental Data for Various Models, Tumbling Mechanisms and Inclusion/Exclusion of Temporal Gradient in Tumbling Probability

Model	Tumbling Probability	Temporal gradient	$\chi_0^{3D} \times 10^4$ (cm^2/s)
RTBL	Eq. 12	$\partial a/\partial t = 0$	2.6
FEM	Eq. 12	$\partial a/\partial t = 0$	1.9
FEM	Eq. 13	$\partial a/\partial t = 0$	3.8
FEM	Eq. 13	$\partial a/\partial t \neq 0$	3.8

model for the chemotactic response used in the cell balance equation. The finite-element solution of the balance equation for one-dimensional gradients represents a substantial economy of computational expense over the cellular dynamics simulations.

A summary of the χ_0^{3D} values obtained using the different models and tumbling probability expressions considered in this article is given in Table 3. Compared to the solution of the balance equation for one-dimensional attractant gradients, RTBL overpredicts the value of the chemotactic sensitivity coefficient by as much as 230% when $\chi_0^{3D} = 105 \times 10^{-4}$ cm^2/s. Values of this magnitude have been reported for conditions under which bacterial growth was limited (Mercer et al., 1993), a situation which is not uncommon in natural environments. It is interesting to note that the use of Eq. 12 for the tumbling probability of *E. coli* as opposed to Eq. 13 leads to an underprediction of the correct value of χ_0^{3D} while the use of the RTBL model as opposed to the balance equation for one-dimensional attractant gradients leads to an overprediction of the correct value of χ_0^{3D}. Therefore, analyses of experimental data for the migration of *E. coli* that use the RTBL model and incorporate Eq. 12 (for example, the studies of Ford and coworkers) contain compensating errors that may result in reasonable values for χ_0^{3D} being inferred from experiment.

Two different responses have been reported for bacteria swimming down an attractant gradient. *E. coli* return to a basal tumbling probability corresponding to what is observed in the absence of a chemical gradient (Berg and Brown, 1972; Brown and Berg, 1974) while *S. typhimurium* increase their tumbling frequency over the basal level when moving down an attractant gradient. Solution of the balance equation for one-dimensional gradients revealed a significant difference in the bacterial density profiles depending on the model used for the tumbling probability, as shown in Figure 7. For bacteria returning to the basal tumbling frequency, the chemotactic response appears less dramatic with respect to the sharpness and intensity of the bands.

Within the SFDC, both a spatial and temporal attractant gradient exist. Prior applications of the RTBL model neglected the temporal gradient arguing that its contribution was small in comparison to the large spatial gradient generated by an initial step change in attractant concentration. Solutions of the balance equation for one-dimensional attractants with and without the temporal gradient showed no significant difference over the range of parameters that were investigated, validating the assumption that the temporal gradient within the material derivative is negligible.

A comparison article to follow will use the numerical solution of the cell balance equation for one-dimensional attractant gradients to interpret experimental data for bacteria responding to simultaneous gradients of two attractants in the same and opposing directions. Hypothetical models for the integration of multiple signals will be evaluated by comparison to experimental results in the SFDC assay.

Acknowledgments

This research was performed by RMF under the sponsorship of the U.S. Dept. of Energy, Environmental Restoration and Waste Management Young Faculty Award Program administered by Oak Ridge Associated Universities. This research was performed by PDF under appointment to the Environmental Restoration and Waste Management Fellowship Program administered by Oak Ridge Associated Universities for the U.S. Dept. of Energy. We thank the reviewers for many helpful and insightful suggestions which formed the basis for the revisions to the manuscript.

Notation

a = attractant concentration (mM)
c = experimentally observed bacterial density (cells/cm^3)
c_i = coefficients in the polynomial approximating the probability distribution of α, the turn angle
D = diffusion coefficient for attractant (cm^2/s)
G = shape functions in the finite-element approximation of n_z
k = probability of turning to a specified direction relative to an initial direction
K = reduced probability of turning to a specified direction relative to an initial direction
K_d = dissociation constant for attractant-receptor binding (mM)
L = length of solution domain in z direction (cm)
$n^{\pm}$ = one-dimensional bacterial density in Segel's equations (cells/cm^3)
n_z = reduced number density of cells in the new model equation (cells/cm^3)
N = number of bacteria
N_b = number of receptors bound to attractant molecules
N_T = number of cell surface receptors
$p^{\pm}$ = probability that a cell moving in the $\pm z$ direction tumbles and becomes a cell moving in the $\mp z$ direction (1/s)
p_r = probability that a bacterium reverses after tumbling
$\vec{r}$ = position vector (cm)
s = one-dimensional cell speed (cm/s)
$\hat{s}$ = unit direction vector
t = time (s)
v = three-dimensional cell speed (cm/s)
x, y, z = coordinate directions

Greek letters

α = angle between a bacterium's direction vector before tumbling and its direction vector after tumbling
β = tumbling probability per unit time (1/s)
γ = interpolation constant in the assumed polynomial for n_z
θ, ϕ = angles of direction of a bacterium
μ = random motility coefficient (cm^2/s)
ν = proportionality constant describing the fractional change in mean = run time per unit time rate of change in cell surface receptors (s)
σ = three-dimensional bacterial probability density (cells/cm^3)
τ = mean bacterial run time (s)
χ = chemotactic sensitivity (cm^2/s)
ψ = average value of cos(α)
ω = implicit/explicit weighting parameter for the finite difference approximation
$\vec{\nabla}_{\vec{r}}$ = divergence operator with respect to $\vec{r}$

Subscripts

0 = in the absence of an attractant or an initial value

Superscripts

+ = positive z-coordinate direction
− = negative z-coordinate direction

Literature Cited

Allaire, P. E., *Basics of the Finite Element Method*, Wm. C. Brown, Dubuque, IA (1985).

Allen, M. P., and D. J. Tildesly, *Computer Simulations of Liquids*, Oxford University Press, New York (1987).

Alt, W., "Biased Random Walk Models for Chemotaxis and Related Diffusion Approximations," *J. Math. Biol.*, **9**, 147 (1980).

Berg, H. C., *Random Walks in Biology*, Princeton University Press, Princeton, NJ (1983).

Berg, H. C., and D. A. Brown, "Chemotaxis in *Escherichia coli* Analysed by Three-dimensional Tracking," *Nature*, **239**, 500 (1972).

Bird, R. B., and H. C. Öttinger, "Transport Properties of Polymeric Liquids," *Ann. Rev. Phys. Chem.*, **43**, 371 (1992).

Brown, D. A., and H. C. Berg, "Temporal Stimulation of Chemotaxis in *E. coli*," *Proc. Natl. Acad. Sci. USA*, **71**, 1388 (1974).

Crank, J., *The Mathematics of Diffusion*, 2nd ed., Clarendon Press, Oxford (1979).

Ford, R. M., and P. T. Cummings, "On the Relationship between Cell Balance Equations for Chemotactic Cell Populations," *SIAM J. Appl. Math.*, **52**, 1426 (1992).

Ford, R. M., and D. A. Lauffenburger, "Measurement of Bacterial Random Motility and Chemotaxis Coefficients: II. Application of Single Cell-Based Mathematical Model," *Biotech. Bioeng.*, **37**, 661 (1991).

Ford, R. M., J. A. Quinn, B. R. Phillips, and D. A. Lauffenburger, "Measurement of Bacterial Random Motility and Chemotaxis Coefficients: I. Stopped-Flow Diffusion Chamber Assay," *Biotech. Bioeng.*, **37**, 647 (1991).

Frymier, P. D., R. M. Ford, and P. T. Cummings, "Cellular Dynamics Simulation of Bacterial Chemotaxis," *Chem. Eng. Sci.*, **48**, 687 (1993).

Keller, E. F., and L. A. Segel, "Model for Chemotaxis," *J. Theor. Biol.*, **30**, 225 (1971).

Lovely, P. S., and F. W. Dalquist, "Statistical Measures of Bacterial Motility and Chemotaxis," *J. Theor. Biol.*, **50**, 477 (1975).

Macnab, R. M., "Sensing the Environment: Bacterial Chemotaxis," *Biological Regulation and Development*, R. Goldberger, ed., Plenum Press, New York, p. 377 (1980).

Macnab, R. M., and D. E. Koshland, "The Gradient-Sensing Mechanism in Bacterial Chemotaxis," *Proc. Natl. Acad. Sci. USA*, **69**, 2509 (1972).

Mercer, J. R., R. M. Ford, J. L. Stitz, and C. Bradbeer, "Growth Rate Effects on Fundamental Transport Properties of Bacterial Populations," *Biotech. and Bioeng.*, **42**, 1277 (1993).

Milton, J. S., and J. C. Arnold, *Introduction to Probability and Statistics: Principles and Applications for Engineering and the Computing Sciences*, McGraw-Hill, New York (1990).

Rivero, M. A., R. T. Tranquillo, H. M. Buettner, and D. A. Lauffenberger, "Transport Models for Chemotactic Cell Populations Based on Individual Cell Behavior," *Chem. Eng. Sci.*, **44**, 2881 (1989).

Segel, L. A., "A Theoretical Study of Receptor Mechanisms in Bacterial Chemotaxis," *SIAM J. Appl. Math.*, **32**, 653 (1977).

Staffeld, P. O., and J. A. Quinn, "Diffusion-Induced Banding of Colloid Particles via Diffusiophoresis: 1. Electrolytes," *J. Coll. Int. Sci.*, **130**, 69 (1989).

Strauss, I., "Bacterial Chemotaxis in the Presence of Multiple Stimuli," Master's thesis, University of Virginia (1992).

Appendix: Direction Change Distribution

The direction change distribution $k(\vec{r}, \hat{s}', t; \hat{s})$ found in Eq. 1 is the probability that a bacterium originally moving in the direction $\hat{s}'$ at time t and at position $\vec{r}$ prior to tumbling moves in the direction $\hat{s}$ after tumbling where $\hat{s} = (\sin\theta\cos\phi, \sin\theta\sin\phi, \cos\theta)$ and $\hat{s}' = (\sin\theta'\cos\phi', \sin\theta'\sin\phi', \cos\theta')$, as shown in Figure 11. Macnab and Koshland (1972) observed

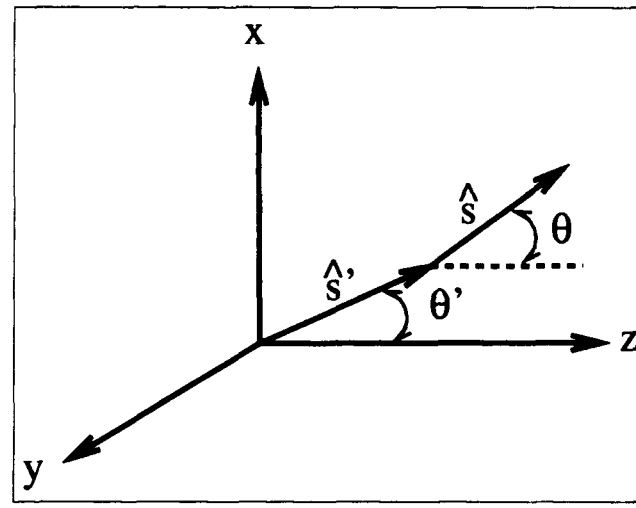

Figure 11. Relationship between the direction vectors, $\hat{s}$ and $\hat{s}'$ and the angles θ and θ'.

experimentally that $k(\vec{r}, \hat{s}', t; \hat{s})$ is independent of the presence of an attractant, so that $k(\vec{r}, \hat{s}', t; \hat{s}) = k(\hat{s}', \hat{s})$. The direction change distribution $K(\theta', \theta)$ found in the balance equation for one-dimensional attractant gradients, Eq. 3, and defined in Eq. A1, is the probability that a bacterium originally moving in a direction with angle θ' off the z-axis prior to tumbling moves in a direction with the angle θ off the z-axis after tumbling. The distributions $k(\hat{s}', \hat{s})$ and $K(\theta', \theta)$ are related by:

$$K(\theta', \theta) = \frac{1}{2\pi}\int_0^{2\pi}\int_0^{2\pi} k(\hat{s}', \hat{s})\, d\phi'\, d\phi \qquad \text{(A1)}$$

Equation A1 gives the relationship between $k(s', s)$ and $K(\theta', \theta)$. The distribution $k(\hat{s}', \hat{s})$ is calculated from the turn angle distribution $p(\alpha)$ where $\cos(\alpha) = \hat{s}\cdot\hat{s}'$. The distribution $p(\alpha)$ was determined experimentally for *E. coli* by Berg and Brown (1972). We used a seventh-order polynomial of the type:

$$p(\alpha) = \sum_{i=1}^{6} c_i \alpha^i (\pi - \alpha)^{7-i} \qquad \text{(A2)}$$

where the c_i are coefficients chosen by the method of least squares to best fit the experimental data for the distribution of turn angles (see also Frymier et al., 1992). The use of the seventh-order polynomial is simply for numerical convenience and does not imply any physical or mechanistic model for the reduced direction change distribution. Since the reduced direction change distribution, $K(\theta', \theta)$, is independent of the attractant concentration and therefore of time, a substantial time savings can be realized if $K(\theta', \theta)$ is tabulated at the control points for two point Gaussian integration on each element so the values can be called on when needed without recalculation.

Manuscript received Mar. 1, 1993, and revision received July 26, 1993.